T cells expressing checkpoint receptor TIGIT are enriched in follicular lymphoma tumors and characterized by reversible suppression of T-cell receptor signaling

Sarah E. Josefsson,[1,2] Kanutte Huse,[1,2] Arne Kolstad,[3] Klaus Beiske,[4] Daniela Pende,[5] Chloé B. Steen,[1,2,6] Else Marit Inderberg,[7] Ole Christian Lingjærde,[1,6] Bjørn Østenstad,[3] Erlend B. Smeland,[1,2] Ronald Levy,[8] Jonathan M. Irish[9,10,11] and June H. Myklebust[1,2]

[1]Centre for Cancer Biomedicine, University of Oslo, Oslo, Norway; [2]Department of Cancer Immunology, Institute for Cancer Research, Oslo University Hospital, Oslo, Norway; [3]Department of Oncology, Division of Cancer Medicine, Oslo University Hospital, Oslo, Norway; [4]Department of Pathology, Oslo University Hospital, Oslo, Norway; [5]Immunology Laboratory, Ospedale Policlinico San Martino, Genova, Italy; [6]Department of Computer Science, University of Oslo, Oslo, Norway; [7]Department of Cellular Therapy, Oslo University Hospital, Oslo, Norway; [8]Division of Oncology, Stanford School of Medicine, Stanford, CA, USA; [9]Department of Cell & Developmental Biology, Vanderbilt University, Nashville, TN, USA; [10]Vanderbilt-Ingram Cancer Center, Vanderbilt University Medical Center, Nashville, TN, USA; [11]Department of Pathology, Microbiology & Immunology, Vanderbilt University Medical Center, Nashville, TN, USA.

Corresponding author:

June H. Myklebust, PhD., Department of Cancer Immunology, Institute for Cancer Research, Oslo University Hospital, Postboks 4953 Nydalen, 0424 Oslo, Norway. Tel (47) 2278 1413; Email: junehm@rr-research.no

Conflict-of-interest disclosure:

The authors declare no potential conflicts of interest.

Running title:

TIGIT is an abundant co-inhibitory receptor in FL

Statement of significance:

TIGIT is a frequently expressed co-inhibitory receptor in CD8 and CD4 T cells from follicular lymphoma tumors. As TIGIT-expressing CD8 FL T cells have impaired TCR signaling and IFN-γ production, TIGIT is a relevant target for therapeutic inhibition.

ABSTRACT

Purpose: T cells infiltrating follicular lymphoma (FL) tumors are considered dysfunctional, yet the optimal target for immune checkpoint blockade is unknown. Characterizing co-inhibitory receptor expression patterns and signaling responses in FL T-cell subsets might reveal new therapeutic targets.

Experimental Design: Surface expression of 9 co-inhibitory receptors governing T-cell function was characterized in T-cell subsets from FL lymph node tumors and from healthy donor tonsils and peripheral blood samples, using high-dimensional flow cytometry. The results were integrated with T-cell receptor (TCR)-induced signaling and cytokine production. Expression of TIGIT ligands were detected by immunohistochemistry.

Results: TIGIT was a frequently expressed co-inhibitory receptor in FL, expressed by the majority of CD8 T effector memory cells, which commonly co-expressed exhaustion markers such as PD-1 and CD244. CD8 FL T cells demonstrated highly reduced TCR-induced phosphorylation (p) of ERK and reduced production of IFN-γ, while TCR proximal signaling (p-CD3ζ, p-SLP76) was not affected. The TIGIT ligands CD112 and CD155 were expressed by follicular dendritic cells in the tumor microenvironment. Dysfunctional TCR signaling correlated with TIGIT expression in FL CD8 T cells, and could be fully restored upon *in vitro* culture. The co-stimulatory receptor CD226 was downregulated in $TIGIT^+$ compared to $TIGIT^-$ CD8 FL T cells, further skewing the balance towards immunosuppression.

Conclusions: TIGIT blockade is a relevant strategy for improved immunotherapy in FL. A deeper understanding of the interplay between co-inhibitory receptors and key T-cell signaling events can further assist in engineering immunotherapeutic regimens to improve clinical outcomes of cancer patients.

Translational relevance

Immunotherapeutic regimens targeting co-inhibitory receptors such as PD-1 have emphasized the role of immune checkpoints in sustaining T-cell immunosuppression. However, the response rate of PD-1 blockade has been lower than anticipated in FL, providing a rationale to investigate the role of other co-inhibitory receptors. Here, in-depth characterization of co-inhibitory receptor expression was combined with functional assessment of intratumor T cells from FL patients. This approach provided new insights into mechanisms that may contribute to immunosuppression in FL by identifying TIGIT as a commonly expressed co-inhibitory receptor in FL T cells, and the expression correlated with reduced effector function. Our results suggest that the potential relevance of TIGIT inhibition as a novel form of checkpoint therapy is high and support clinical investigation of TIGIT blockade in FL, possibly in combination with blockade of PD-1.

INTRODUCTION

Follicular lymphoma (FL) is the most common subtype of indolent non-Hodgkin lymphoma. Although outcomes have improved (1), current chemo-immunotherapy regimens are usually not curative. Additionally, FL patients can transform to more aggressive histology, leading to rapid progression and need for intensive therapy (2). Ongoing clinical trials to improve treatment of FL focus on novel targeted agents and various immunomodulatory regimens, including immunotherapy with checkpoint blockade (3,4).

Targeting co-inhibitory receptors such as PD-1 and CTLA-4 by immune checkpoint blockade can restore the function of exhausted T cells with anti-tumor reactivity (5,6). T cells in the FL tumor microenvironment (TME) are considered dysfunctional and associated with disease progression (7-9). However, whereas blockade of PD-1 represents a breakthrough for several solid cancers (10-12) and for Hodgkin's lymphoma (13), the response rate as monotherapy in FL has been lower than anticipated (14), given the high expression of PD-1 in intra-tumor T cells and presence of PD-L1^{+} histiocytes in the TME (9,15). However, the influence of different T-cell subsets for lymphomagenesis is complex. While T follicular helper cells (T_{FH}) display PD-1^{hi} phenotype and are highly functional by supporting lymphoma B cells through CD40 ligand and secretion of cytokines IL-4 and IL-21 (16-18), exhausted T cells express intermediate levels of PD-1 (15,19). A hallmark of T-cell exhaustion is expression of multiple co-inhibitory receptors alongside progressive loss of effector functions (20). Therefore, co-blockade of several co-inhibitory receptors might be necessary to achieve optimal anti-tumor T-cell responses. T cell immunoglobulin and ITIM domain (TIGIT) is a recently identified co-inhibitory receptor, expressed by natural killer (NK) cells, effector T cells (T_E), T regulatory cells (T_{regs}) and T_{FH} (21-25). Prior findings suggest TIGIT as a candidate for checkpoint blockade, as TIGIT is frequently found on tumor-infiltrating T cells (TILs) in solid tumors and in AML (26-28), and the TIGIT ligands, CD155 and CD112, are expressed by different cell types including antigen presenting cells and tumor cells (21,22,24,29).

Numerous genes are recurrently mutated in FL (30-33), creating tumor antigens, including the lymphoma immunoglobulins, that may trigger T-cell anti-tumor responses (34). Antigen recognition by the T-cell receptor (TCR) initiates a cascade of tyrosine phosphorylations, and the amplitude and duration of TCR signaling is critical for T-cell effector function (35). Hence, exhausted T cells can be distinguished from functional T cells by low TCR signaling

strength. Upon TCR interaction with peptide-MHC, the immunoreceptor tyrosine-based activation motifs (ITAMs) of the TCR associated CD3 subunits become phosphorylated by Src family kinases such as LCK (35,36). Subsequent recruitment and phosphorylation of the adaptor protein SH2-domain containing leukocyte protein of 76 kDa (SLP76), and linker for activation of T cells (LAT), results in formation of the LAT signalosome which enables activation of multiple downstream effectors, including activation of the RAS-MEK-ERK, PI3K/AKT and NF-κB pathways. TCR signaling is enhanced by co-stimulatory receptors such as CD28, but dampened by co-inhibitory receptors such as CTLA-4 and PD-1 due to recruitment of phosphatases (37,38).

The hypothesis underlying this study was that characterizing signaling responses and co-inhibitory receptor expression in intra-tumor T-cell subsets could reveal new targets for immune checkpoint blockade. Based on previous studies, demonstrating the importance of PD-1 for T-cell immunosuppression (9), our approach was to measure functional responses in T cells with differential expression of PD-1, while in parallel screening for co-inhibitory receptors that could be of interest for immune checkpoint blockade in combination with PD-1. This approach identified TIGIT as the most frequently expressed co-inhibitory receptor in FL T cells, and the expression was associated with T-cell dysfunction. Taken together, our data suggest TIGIT as a promising new target for immune checkpoint blockade in FL.

MATERIALS AND METHODS

Human samples

Specimens were obtained with informed consent in accordance with the Declaration of Helsinki and with approval from the Regional Committees for Medical and Health Research Ethics (REK S-0749b and 2010/1147a). Malignant LN specimens were obtained at time of diagnosis from FL patients (n = 12) or after treatment (n = 2) at the Norwegian Radium Hospital, Oslo, Norway, and tonsils were obtained from patients undergoing tonsillectomy at Agroklinikken (Asker, Norway). LN and tonsils were processed to single cell suspensions by mincing and stored as aliquots in liquid nitrogen. Peripheral blood was collected from anonymous, healthy donors at The Blood Bank in Oslo (REK S-03280), processed to mononuclear cells (PBMC) by Ficoll gradient centrifugation (Ficoll-Paque™ PLUS, GE Healthcare, NJ, USA) and cryopreserved in liquid nitrogen.

Reagents

Stimulation reagents: TCR activation (α-TCR): anti-CD3 biotin and anti-CD28 biotin were used at 5 ug/mL each and avidin (Thermo Fischer Scientific) was used at 50 µg/mL. Phorbol 12-myristate 13-acetate (PMA) was used at 125 ng/mL and ionomycin was used at 500 ng/mL (Sigma-Aldrich). GolgiPlug was from BD Biosciences. Cells were stained using fluorochrome-coupled antibodies (Supplementary Table 1). Antibody used to detect FoxP3 was added after fixation and permeabilization according to the eBioscience protocol. Brilliant Stain Buffer (BD biosciences) was used as staining buffer. Pacific Blue used for fluorescent barcoding of cells was from Life Technologies, Molecular probes.

Activation of T-cell signaling and phospho-specific flow cytometry

Activation of signaling and detection by phospho-specific flow cytometry was performed as described (9,39,40). Specimens were thawed and cells were allowed to rest at 37°C for 4h, before redistribution into v-bottomed 96 well plates and given another 20 minutes rest. For functional studies over time, cells were cultured for 48h at 37°C, at 2.5 x 10^6/mL in CellGro DC (CellGenix) supplemented with 5% human serum (Diaserve Laboratories). 20 U/mL IL-2 (Chiron) was added in some experiments as specified. Signaling was activated by α-TCR for 1, 4 or 10 minutes (details in Supplementary methods). Signaling was stopped by adding paraformaldehyde (PFA; 1.6%), followed by centrifugation and permeabilization in >90% freezer-cold methanol. After rehydration, the cells were stained with antibodies, or

"barcoded" with Pacific Blue prior to staining with antibodies as previously described (9). The samples were collected on a LSR II flow cytometer (BD Biosciences). Data was analyzed using Cytobank Software, https://community.cytobank.org. Relative phosphorylation changes (fold changes) were calculated using arcsinh transformation of median fluorescence intensity (MFI) of the cell population of interest.

viSNE analysis

The computational tool viSNE (41) was used for visualization of immunophenotype data, see supplementary methods.

Stimulation of cytokine production

Samples were incubated for 6h in the presence of PMA and ionomycin, with GolgiPlug present for the last 4h. PFA (1.6%) was added to stop activity, followed by centrifugation and permeabilization in >90% freezer-cold methanol. At this point, the samples could be stored at -80°C, before staining with antibodies and flow cytometry acquisition.

Gene expression analysis

Gene expression data were obtained from two different datasets; Dave et al. (7) and Brodtkorb et al. (42), and included pre-treatment FL biopsies only, see supplementary methods.

Immunohistochemistry

Serial sections of cryopreserved FL tissue were stained with antibodies for CD155 (L95) and CD112 (L14) as previously described (43), in addition to CD21 (2G9).

RESULTS

FL CD8 T-cell composition is skewed towards PD-1^{int} phenotype

To explore if PD-1 was more frequently expressed in intra-tumor T cells from FL than in corresponding subsets from healthy tissues, LN specimens from 14 FL patients were immunophenotyped and compared with 11 tonsillar and 7 PBMC samples from healthy donors. In order to distinguish T_{FH} from other subsets, distribution of T cells was characterized based on differential expression of PD-1 and ICOS in CD4 (PD-1^{-}ICOS^{-}, PD-1^{int}ICOS^{-}, PD-1^{int}ICOS^{+}, and PD-1^{hi}ICOS^{+} (T_{FH})) and CD8 (PD-1^{-}ICOS^{-} and PD-1^{int}ICOS^{-}) T-cell subsets (Fig. 1A). We found that neither the T_{FH} compartment nor the CD4^{+} PD-1^{int} T-cell subsets were significantly different between FL tumors and tonsil controls. In contrast, the CD8^{+} PD-1^{int} subset was markedly increased in FL tumors compared to healthy PBMC or tonsils ($p < 0.003$ and $p < 0.0001$, Fig. 1B), suggesting a larger fraction of exhausted CD8 T cells in FL.

CD8 T cells from FL display reduced IFN-γ production

We next measured cytokine production in relation to PD-1 expression in CD4 and CD8 T cells. We observed that reduced percentage of CD8 T cells from FL patients produced IFN-γ, compared to healthy individuals. Interestingly, IFN-γ production was reduced in PD-1^{-} as well as PD-1^{int} CD8 T cells (Fig. 1C), indicating that PD-1-negative CD8 FL T cells were also suppressed. This finding suggests presence of other inhibitory mechanisms in PD-1^{-} CD8 FL T cells, leading to reduced functionality. Production of IL-4 and IL-21 was also measured, but was not significantly different in CD8 T cells from FL LN and healthy donors (Supplementary Fig. S1). In CD4 T cells, IL-4 production was low but at comparable levels in FL and tonsillar subsets, whereas IL-21 production was reduced in all FL subsets except for PD-1^{-}ICOS^{-} cells (Supplementary Fig. S1).

TCR-induced p-ERK is highly reduced in FL T cells

As functional TCR signaling is critical for generation of effective anti-tumor T-cell responses, including production of IFN-γ, we next investigated TCR-induced signaling in T cells from FL tumors (Fig. 2A). TCR signaling was activated using α-CD3 and α-CD28 biotinylated antibodies, followed by avidin crosslinking. To identify optimal time points to detect maximal phosphorylation levels, TCR was activated for 1, 4 and 10 minutes. Whereas p-CD3ζ and p-SLP76 peaked at 1 minute post stimulation, p-ERK signaling was undetectable at 1 minute

and reached the maximal level 4 minutes after stimulation (Supplementary Fig. S2). A comparison of TCR-induced signaling responses in FL and healthy individuals revealed that T cells from FL patients were distinguished by highly reduced TCR-induced p-ERK, while p-SLP76 and p-CD3ζ levels were comparable (Fig. 2B). The low levels of TCR-induced p-ERK was evident in $CD8^{+}PD\text{-}1^{int}$ FL T cells, with a relative median fold change (FC) of 0.18 as compared to 0.56 and 0.34 in PBMC and tonsils, respectively (Fig. 2C). Strikingly, TCR-induced p-ERK was low in all CD4 FL T-cell subsets (range 0.2-0.4; Fig. 2C). In contrast, TCR proximal signaling, as determined by p-SLP76, was comparable in FL and tonsillar T cells, with median FC ranges of 1.7-2.0 and 1.9-2.2, respectively (Fig. 2C). Phosphorylation of CD3ζ was also potent in FL, similar to the levels observed in tonsillar T-cell subsets (Fig. 2C). Interestingly, the low TCR-induced p-ERK observed across all T-cell subsets from FL LN indicated a block in the distal part of the pathway. This corresponded with the observed reduction in IFN-γ production.

TIGIT is frequently expressed in T cells from FL

We hypothesized that multiple co-inhibitory receptors might play a role in dampening T-cell anti-tumor responses in FL. We therefore used 11-parameter flow cytometry panels to achieve an in-depth characterization of co-inhibitory receptor expression patterns in FL T-cell subsets, and compared patterns with healthy donor samples as before. A viSNE analysis, based on the expression of 6 lineage markers (CD4, CD8, CXCR5, ICOS, CD45RA and CCR7) was used to visualize the data and to identify conventional T-cell subsets, as well as T-cell subsets identified based on PD-1 and ICOS expression (Supplementary Fig. S3A-C). The expression pattern of 9 co-inhibitory receptors; PD-1, TIGIT, TIM-3, CTLA-4, LAG-3, BTLA, CD244, LAIR-1 and CD160 was then identified in the conventional T-cell subsets (Fig. 3). Strikingly, TIGIT was an abundant co-inhibitory receptor in FL T cells, and was expressed by the majority of CD4 and CD8 T effector memory (T_{EM}) cells (Fig. 3). Furthermore, $TIGIT^{+}$ CD8 T_{EM} cells from FL co-expressed several exhaustion markers, such as PD-1 and CD244 (Fig. 3, Supplementary Fig. S3D-E), suggesting that TIGIT marks exhausted CD8 T cells in FL.

Detailed analysis revealed that TIGIT was expressed at significantly higher levels across all T-cell subsets in FL tumors compared to healthy donor tonsils or PBMC, but with contrasting expression pattern across distinct subsets: low expression in naive T cells and highest in T_{EM} and T_{FH} cells. In average 80% and 79% of CD8 and CD4 T_{EM} cells from FL expressed TIGIT (Figure 4A-C). This is an important finding as T_{EM} was the major subset of CD4 and CD8 T

cells in FL tumors (Supplementary Fig. S4). The majority of FL CD8 and CD4 T_{EM} cells also expressed PD-1 (80% and 65%, respectively), and some expressed BTLA (10% and 42%, Fig. 4B-C). TIM-3, CTLA-4, LAG-3, LAIR-1 and CD160 were all less frequently expressed in FL CD4 and CD8 T_{EM} cells (in average <25%; Supplementary Fig. S5). CD244 was expressed by 57% of CD8 T_{EM}, similar to tonsils (Supplementary Fig. S5). As T_{regs} also can express several co-inhibitory receptors, TIGIT expression was investigated in $CD4^+CD25^+FOXP3^+$ T_{regs} from FL LN and from healthy samples. Remarkably, TIGIT was expressed by the vast majority of FL T_{regs} (range 92-99%). This was not tumor specific, as most T_{regs} from healthy tonsils and PBMC expressed TIGIT (Fig. 4D). The $TIGIT^+$ T_{regs} accounted for in average 25% of the $TIGIT^+$ CD4 T cells in FL (Supplementary Fig. S6). Together, these results identified TIGIT and PD-1 as the most frequently expressed co-inhibitory receptors in FL T cells.

Expression of CD112, CD155 and CD226 in FL

TIGIT exerts inhibitory functions upon interaction with its ligands, CD112 or CD155 (22). Immunophenotypic analysis of FL specimens showed that less than 5% of the tumor cells expressed CD155 or CD112 (Supplementary Table 2). Importantly, although not expressed by malignant B cells, immunohistochemical staining of 6 samples of FL revealed expression of CD155 and CD112 on follicular dendritic cells (FDC) within the neoplastic follicles, and on endothelial cells (Fig. 5A). Additionally, transcriptional analysis using two different gene expression profiling datasets (7,42) showed that CD112 and CD155 are present in FL, and further confirmed TIGIT as the most highly expressed co-inhibitory receptor (Supplementary Fig. S7).

Since TIGIT competes for ligand binding with the co-stimulatory receptor CD226 (24,44), co-staining for the two receptors to identify their relationship in FL T cells was performed. Interestingly, while $TIGIT^+$ CD8 T cells from healthy donor PBMC had a substantial proportion of cells that co-expressed both receptors, few $TIGIT^+$ CD8 T cells from FL tumors expressed the co-stimulatory receptor compared to $TIGIT^-$ CD8 FL T cells ($p < 0.02$, by Wilcoxon test, Fig. 5B). Expression of CD226 was particularly low in CD8 T_{EM} cells (Fig. 5C), which displayed the highest expression of TIGIT (Fig. 4B). In contrast, CD226 was frequently expressed in $TIGIT^+$ CD4 T cells in FL, including T_{FH} cells (Fig. 5B-C). Together, this indicates an imbalance in the TIGIT/CD226 axis in CD8 FL T cells.

$TIGIT^+$ CD8 T cells display TCR distal signaling defects that can be restored

To further investigate the relationship between TIGIT expression and dysfunctional TCR-induced signaling, we included detection of TIGIT in our signaling assay. Distinguishing between TIGIT$^-$ and TIGIT$^+$ cells among the CD8 FL T cells revealed that TIGIT$^+$ cells had reduced TCR-induced p-ERK compared to TIGIT$^-$ cells (Fig. 6A-B). This contrasted TCR proximal signaling, demonstrated by high levels of TCR-induced p-SLP76 regardless of TIGIT expression (Fig. 6B). These results indicate that TIGIT plays a role in dampening signaling distal to the TCR.

To test whether the dysfunctional TCR signaling could be restored, we studied signaling responses after 48h *in vitro* culture (Fig. 6C). Detection of TIGIT revealed that the percentage of TIGIT$^+$ CD8 FL T cells was stable over time (Supplementary Fig. S8). Interestingly, while TCR-induced p-SLP76 was comparable in CD8 T cells at day 0 and after 2 days, we observed a striking increase in TCR-induced p-ERK, from 1.03 to 2.01 FC (Fig. 6D). Importantly, the recovery of TCR-induced p-ERK was highly reproducible and remarkably high in TIGIT$^+$ CD8 FL T cells (median fold change from 0.8 at day 0 to 2.1 at day 2) as compared to TIGIT$^-$ CD8 FL T cells (from 1.6 at day 0 to 2.7 at day 2) (Fig. 6E-F; Supplementary Fig. S9). As TIGIT ligands were expressed by FDC (Fig. 5A) which are tightly adhered to the stroma, these cells were not preserved and are therefore not present in the cryopreserved single cell suspensions used in the functional assays. In conclusion, our results showed that the highly reduced TCR-induced p-ERK in FL could be recovered upon *in vitro* culture when TIGIT ligand-expressing cells are not present, suggesting that FL T cells receive suppressive signals through TIGIT via ligand$^+$ cells in the TME *in vivo*.

DISCUSSION

Immune checkpoint blockers have shown impressive clinical benefits in several tumor types. Despite frequent expression of PD-1 in intra-tumor T cells in FL (9,15), a significant proportion of patients do not respond to anti-PD-1 blockade (14,45). Tumor genomic landscape, mutational load and tumor specific neoantigens are potential determinants of the response to immune checkpoint blockade, as well as characteristics of the TME (34,46-49). As T-cell exhaustion might relate to co-expression of several co-inhibitory receptors, identification of the most relevant types as targets for immune checkpoint blockade in FL patients will be important in order to fully unleash the anti-tumor response. In this study, we performed a multi-dimensional functional and phenotypical characterization of intra-tumor T cells from FL patients and compared with tonsils and PBMC from healthy donors to identify relevant targets for immune checkpoint blockade in FL. This approach identified TIGIT and PD-1 as the most frequently expressed co-inhibitory receptors. In FL CD8 T cells, we observed reduced production of IFN-γ as well as highly reduced TCR-induced p-ERK, which correlated with TIGIT expression and could be fully restored by *in vitro* culture in absence of TIGIT ligands CD155 and CD112. The TIGIT ligands were expressed by FDC and endothelial cells in FL tumors. Together, these results indicate that TIGIT is a relevant target for immune checkpoint blockade in FL.

Strikingly, our results showed that TIGIT in average was expressed in more than 80% of CD8 and CD4 T_{EM} cells from FL tumors, which accounted for 50% and 60% of CD8 and CD4 T cells, respectively. Furthermore, more than 95% of T_{regs} and T_{FH} cells from FL LN expressed TIGIT. Importantly, TIGIT might potentially have divergent functions in different T-cell subsets. Agonistic anti-TIGIT antibody had direct inhibitory effects on T-bet expression and IFN-γ production in $CD4^+$ T_E cells (50), and loss of TIGIT *in vivo* increased T-cell proliferation and proinflammatory cytokine production (25). In contrast to the unresponsive phenotype of $TIGIT^+$ T_E cells, $TIGIT^+$ T_{regs} are highly functional cells. Several studies have demonstrated that $TIGIT^+$ T_{regs} have increased expression of effector molecules and are more potent suppressors of T_E proliferation than $TIGIT^-$ T_{regs} (28,51,52). As the frequency of T_{regs} is increased in FL LN, $TIGIT^+$ T_{regs} are likely to contribute to sustained immune suppression in FL. In addition, TIGIT is frequently expressed by tonsillar T_{FH} (53), and we observed that the majority (>95%) of T_{FH} from FL LN as well as tonsils from healthy donors expressed TIGIT. Previous studies suggest that TIGIT mediates adhesion of T_{FH} to FDC in germinal centers

(23), and TIGIT is required for efficient B-cell helper function of peripheral blood circulating T_{FH} (54). Furthermore, TIGIT can outcompete the co-stimulatory receptor CD226 due to its higher affinity for the same ligand and by blocking dimerization of CD226, thus preventing its co-stimulatory function (21,44,50,55). Our results revealed that TIGIT$^+$ CD8 FL T cells rarely expressed the competing co-stimulatory receptor. This indicated an imbalance between co-stimulation and co-inhibition in these cells, further suggesting that TIGIT plays a role in dampening CD8 T-cell anti-tumor responses in FL. Altogether, this suggests that immune checkpoint blockade targeting TIGIT should enable highly potent T-cell anti-tumor responses in several ways, including restoring anti-tumor potential of T effector cells, dampening the T_{reg} immunosuppressive effect and by reducing the tumor supporting effects of T_{FH} cells. In addition to the direct effects of TIGIT in T cells, TIGIT can directly restrain NK cell activity (56) and indirectly exert inhibitory effects by activating immunoregulatory dendritic cells upon ligand interaction (21). Hence, blocking TIGIT in these cells may also be pivotal for efficient immunotherapy responses.

By combined detection of TIGIT, T-cell markers and phosphorylation of signaling effectors post TCR activation, we identified a clear correlation between TIGIT expression and TCR signaling dysfunction in CD8 FL T cells. However, TIGIT needs to be ligated to exert its suppressive function. Our results showed that less than 5% of FL tumor cells expressed the TIGIT ligands CD155 and CD112. Instead, immunohistochemical staining revealed the presence of CD155 and CD112 on FDC and on endothelial cells in FL tumors. These cells are tightly adhered to the stroma and were not detectable in the cryopreserved samples used for immunophenotyping by flow cytometry. However, the ligand$^+$ FDC are likely to interact with TIGIT-expressing T cells *in vivo*, thereby preventing potent anti-tumor T-cell responses in FL. We were not able to provide direct proof for this hypothesis, but further support comes from the *in vitro* cultures of FL T cells. When cultured in the absence of CD155$^+$ or CD112$^+$ cells, CD8 TIGIT$^+$ FL T cells could regain their TCR signaling capacity. Based on this, we cannot exclude the possibility that culture of FL derived CD8 T cells over time also removes other suppressive signals, as demonstrated by effectiveness of TIL therapy in FL (57). Although the mechanisms underpinning how TIGIT modulates T-cell intrinsic signaling is poorly understood, studies in NK cells suggest that TIGIT upon ligation recruits the inositol 5-phosphatase SHIP1 to attenuate signaling downstream of SLP76, leading to dephosphorylation of ERK and subsequent inhibition of IFN-γ production (58,59). This is in agreement with what we observed in FL T cells; that TIGIT expression correlated with highly

reduced TCR-induced p-ERK that translated into reduced IFN-γ production in CD8 FL T cells, while phosphorylation of CD3ζ and SLP76 remained unaffected and similar to healthy control T cells. Our hypothesis, that low TCR-induced p-ERK marks dysfunctional T cells in FL, is further supported by the current understanding that impaired activation of ERK is an indicator of T-cell anergy. This is based on observations showing that uncoupling of the ERK pathway is an important underlying mechanism in antigenic unresponsiveness of T cells. Antigen recognition under suboptimal conditions, such as lack of co-stimulation or upregulation of co-inhibitory receptors, can act to disrupt TCR-induced p-ERK, hence resulting in poor T-cell effector function (60,61).

While TIGIT can recruit SHIP1 to modulate cell function, PD-1 blocks signaling events downstream of the TCR by recruiting the protein tyrosine phosphatases SHP1 and SHP2. These phosphatases can inhibit phosphorylation of signaling effectors both proximal and distal to the TCR (62-64). In fact, we found low levels of TCR-induced p-ERK to be associated with TIGIT as well as PD-1 expression. This indicates that TIGIT and PD-1 may both contribute to the dysfunctional TCR-induced signaling observed in FL, potentially by recruitment of different phosphatases. In context with the finding that TIGIT and PD-1 were the two major co-inhibitory receptors, and often co-expressed by FL T cells, this provides a rationale for co-blockade of these receptors to improve T-cell activity and tumor killing. Although not yet explored in lymphoma, co-blockade of TIGIT and PD-1 has generated promising results from pre-clinical studies in other cancer types. Combined blockade of the two receptors led to complete responses in tumor mouse models of breast and colorectal cancer, while blocking only one receptor had little effect (27). Furthermore, co-blockade of PD-1 and TIGIT led to increased IFN-γ production in CD8 TILs from melanoma patients, and TIGIT blockade was able to restore cytokine production in CD8 T cells from AML patients (26,65).

In conclusion, our results provide new insights into mechanisms that may contribute to immune suppression in FL. In-depth mapping of co-inhibitory receptor expression and functional assessment in distinct T-cell subtypes will enhance our biological understanding for the complex regulation of anti-tumor T-cell responses, and exploiting this further in relation to immune checkpoint blockade is needed to further enhance the precision of this therapy.

ACKNOWLEDGEMENTS

We thank Eva Kimby for critial review of the manuscript.

GRANT SUPPORT

This work was supported by the Research Council of Norway (FRIMEDBIO 230817/F20; S.E. Josefsson), and Centre of Excellence (Centre for Cancer Biomedicine; J.H. Myklebust and E.B. Smeland), the Norwegian Cancer Society (162948; K. Huse, 163151; E.B. Smeland, and 162844; J.H. Myklebust), and Associazione Italiana per la Ricerca sul Cancro (AIRC IG-16764; D. Pende).

AUTHORSHIP

Contributions: S.E.J., K.H., E.B.S., R.L., J.M.I. and J.H.M. designed the research. S.E.J. and K.H. performed experiments. S.E.J., K.H., C.B.S., O.C.L., J.M.I. and J.H.M. analyzed data. K.B. performed immunohistochemical analysis. D.P. generated mAb L95 and L14. E.M.I designed culture conditions. A.K. and B.Ø. provided patient samples and clinical data. S.E.J., K.H. and J.H.M. wrote the paper, and all authors approved the final manuscript.

REFERENCES

1. Tan D, Horning SJ, Hoppe RT, Levy R, Rosenberg SA, Sigal BM, *et al.* Improvements in observed and relative survival in follicular grade 1-2 lymphoma during 4 decades: the Stanford University experience. Blood 2013;122(6):981-7.
2. Link BK, Maurer MJ, Nowakowski GS, Ansell SM, Macon WR, Syrbu SI, *et al.* Rates and outcomes of follicular lymphoma transformation in the immunochemotherapy era: a report from the University of Iowa/MayoClinic Specialized Program of Research Excellence Molecular Epidemiology Resource. J Clin Oncol 2013;31(26):3272-8.
3. Nowakowski GS, Ansell SM. Therapeutic targeting of microenvironment in follicular lymphoma. Hematology Am Soc Hematol Educ Program 2014;2014(1):169-73.
4. Maddocks K, Barr PM, Cheson BD, Little RF, Baizer L, Kahl BS, *et al.* Recommendations for Clinical Trial Development in Follicular Lymphoma. J Natl Cancer Inst 2017;109(3).
5. Topalian SL, Drake CG, Pardoll DM. Immune checkpoint blockade: a common denominator approach to cancer therapy. Cancer Cell 2015;27(4):450-61.
6. Armand P. Immune checkpoint blockade in hematologic malignancies. Blood 2015;125(22):3393-400.

7. Dave SS, Wright G, Tan B, Rosenwald A, Gascoyne RD, Chan WC, *et al.* Prediction of survival in follicular lymphoma based on molecular features of tumor-infiltrating immune cells. N Engl J Med 2004;351(21):2159-69.
8. Ramsay AG, Clear AJ, Kelly G, Fatah R, Matthews J, Macdougall F, *et al.* Follicular lymphoma cells induce T-cell immunologic synapse dysfunction that can be repaired with lenalidomide: implications for the tumor microenvironment and immunotherapy. Blood 2009;114(21):4713-20.
9. Myklebust JH, Irish JM, Brody J, Czerwinski DK, Houot R, Kohrt HE, *et al.* High PD-1 expression and suppressed cytokine signaling distinguish T cells infiltrating follicular lymphoma tumors from peripheral T cells. Blood 2013;121(8):1367-76.
10. Topalian SL, Hodi FS, Brahmer JR, Gettinger SN, Smith DC, McDermott DF, *et al.* Safety, activity, and immune correlates of anti-PD-1 antibody in cancer. N Engl J Med 2012;366(26):2443-54.
11. Postow MA, Chesney J, Pavlick AC, Robert C, Grossmann K, McDermott D, *et al.* Nivolumab and ipilimumab versus ipilimumab in untreated melanoma. N Engl J Med 2015;372(21):2006-17.
12. Brahmer J, Reckamp KL, Baas P, Crino L, Eberhardt WE, Poddubskaya E, *et al.* Nivolumab versus Docetaxel in Advanced Squamous-Cell Non-Small-Cell Lung Cancer. N Engl J Med 2015;373(2):123-35.
13. Ansell SM, Lesokhin AM, Borrello I, Halwani A, Scott EC, Gutierrez M, *et al.* PD-1 blockade with nivolumab in relapsed or refractory Hodgkin's lymphoma. N Engl J Med 2015;372(4):311-9.
14. Lesokhin AM, Ansell SM, Armand P, Scott EC, Halwani A, Gutierrez M, *et al.* Nivolumab in Patients With Relapsed or Refractory Hematologic Malignancy: Preliminary Results of a Phase Ib Study. J Clin Oncol 2016;34(23):2698-704.
15. Yang ZZ, Grote DM, Ziesmer SC, Xiu B, Novak AJ, Ansell SM. PD-1 expression defines two distinct T-cell sub-populations in follicular lymphoma that differentially impact patient survival. Blood Cancer J 2015;5:e281.
16. Pangault C, Ame-Thomas P, Ruminy P, Rossille D, Caron G, Baia M, *et al.* Follicular lymphoma cell niche: identification of a preeminent IL-4-dependent T(FH)-B cell axis. Leukemia 2010;24(12):2080-9.
17. Ame-Thomas P, Le Priol J, Yssel H, Caron G, Pangault C, Jean R, *et al.* Characterization of intratumoral follicular helper T cells in follicular lymphoma: role in the survival of malignant B cells. Leukemia 2012;26(5):1053-63.
18. Ame-Thomas P, Hoeller S, Artchounin C, Misiak J, Braza MS, Jean R, *et al.* CD10 delineates a subset of human IL-4 producing follicular helper T cells involved in the survival of follicular lymphoma B cells. Blood 2015;125(15):2381-5.
19. Smeltzer JP, Jones JM, Ziesmer SC, Grote DM, Xiu B, Ristow KM, *et al.* Pattern of CD14+ follicular dendritic cells and PD1+ T cells independently predicts time to transformation in follicular lymphoma. Clin Cancer Res 2014;20(11):2862-72.
20. Wherry EJ, Kurachi M. Molecular and cellular insights into T cell exhaustion. Nat Rev Immunol 2015;15(8):486-99.
21. Yu X, Harden K, Gonzalez LC, Francesco M, Chiang E, Irving B, *et al.* The surface protein TIGIT suppresses T cell activation by promoting the generation of mature immunoregulatory dendritic cells. Nat Immunol 2009;10(1):48-57.
22. Stanietsky N, Simic H, Arapovic J, Toporik A, Levy O, Novik A, *et al.* The interaction of TIGIT with PVR and PVRL2 inhibits human NK cell cytotoxicity. Proc Natl Acad Sci USA 2009;106(42):17858-63.

23. Boles KS, Vermi W, Facchetti F, Fuchs A, Wilson TJ, Diacovo TG, *et al.* A novel molecular interaction for the adhesion of follicular CD4 T cells to follicular DC. Eur J Immunol 2009;39(3):695-703.
24. Levin SD, Taft DW, Brandt CS, Bucher C, Howard ED, Chadwick EM, *et al.* Vstm3 is a member of the CD28 family and an important modulator of T-cell function. Eur J Immunol 2011;41(4):902-15.
25. Joller N, Hafler JP, Brynedal B, Kassam N, Spoerl S, Levin SD, *et al.* Cutting edge: TIGIT has T cell-intrinsic inhibitory functions. J Immunol 2011;186(3):1338-42.
26. Chauvin JM, Pagliano O, Fourcade J, Sun Z, Wang H, Sander C, *et al.* TIGIT and PD-1 impair tumor antigen-specific CD8(+) T cells in melanoma patients. J Clin Invest 2015;125(5):2046-58.
27. Johnston RJ, Comps-Agrar L, Hackney J, Yu X, Huseni M, Yang Y, *et al.* The immunoreceptor TIGIT regulates antitumor and antiviral CD8(+) T cell effector function. Cancer Cell 2014;26(6):923-37.
28. Kurtulus S, Sakuishi K, Ngiow SF, Joller N, Tan DJ, Teng MW, *et al.* TIGIT predominantly regulates the immune response via regulatory T cells. J Clin Invest 2015;125(11):4053-62.
29. Casado JG, Pawelec G, Morgado S, Sanchez-Correa B, Delgado E, Gayoso I, *et al.* Expression of adhesion molecules and ligands for activating and costimulatory receptors involved in cell-mediated cytotoxicity in a large panel of human melanoma cell lines. Cancer Immunol Immunother: CII 2009;58(9):1517-26.
30. Green MR, Gentles AJ, Nair RV, Irish JM, Kihira S, Liu CL, *et al.* Hierarchy in somatic mutations arising during genomic evolution and progression of follicular lymphoma. Blood 2013;121(9):1604-11.
31. Okosun J, Bodor C, Wang J, Araf S, Yang CY, Pan C, *et al.* Integrated genomic analysis identifies recurrent mutations and evolution patterns driving the initiation and progression of follicular lymphoma. Nat Genet 2014;46(2):176-81.
32. Pasqualucci L, Khiabanian H, Fangazio M, Vasishtha M, Messina M, Holmes AB, *et al.* Genetics of follicular lymphoma transformation. Cell Rep 2014;6(1):130-40.
33. Green MR, Kihira S, Liu CL, Nair RV, Salari R, Gentles AJ, *et al.* Mutations in early follicular lymphoma progenitors are associated with suppressed antigen presentation. Proc Natl Acad Sci USA 2015;112(10):E1116-25.
34. Khodadoust MS, Olsson N, Wagar LE, Haabeth OA, Chen B, Swaminathan K, *et al.* Antigen presentation profiling reveals recognition of lymphoma immunoglobulin neoantigens. Nature 2017;543(7647):723-7.
35. Brownlie RJ, Zamoyska R. T cell receptor signalling networks: branched, diversified and bounded. Nature Rev Immunol 2013;13(4):257-69.
36. Malissen B, Gregoire C, Malissen M, Roncagalli R. Integrative biology of T cell activation. Nat Immunol 2014;15(9):790-7.
37. Acuto O, Di Bartolo V, Michel F. Tailoring T-cell receptor signals by proximal negative feedback mechanisms. Nat Rev Immunol 2008;8(9):699-712.
38. Chen L, Flies DB. Molecular mechanisms of T cell co-stimulation and co-inhibition. Nature Revi Immunol 2013;13(4):227-42.
39. Irish JM, Myklebust JH, Alizadeh AA, Houot R, Sharman JP, Czerwinski DK, *et al.* B-cell signaling networks reveal a negative prognostic human lymphoma cell subset that emerges during tumor progression. Proc Natl Acad Sci USA 2010;107(29):12747-54.
40. Myklebust JH, Brody J, Kohrt HE, Kolstad A, Czerwinski DK, Walchli S, *et al.* Distinct patterns of B-cell receptor signaling in non-Hodgkins' lymphomas identified by single cell profiling. Blood 2017; 129(6):759-770.

41. Amir el AD, Davis KL, Tadmor MD, Simonds EF, Levine JH, Bendall SC, *et al.* viSNE enables visualization of high dimensional single-cell data and reveals phenotypic heterogeneity of leukemia. Nat Biotechnol 2013;31(6):545-52.
42. Brodtkorb M, Lingjaerde OC, Huse K, Troen G, Hystad M, Hilden VI, *et al.* Whole-genome integrative analysis reveals expression signatures predicting transformation in follicular lymphoma. Blood 2014;123(7):1051-4.
43. Pende D, Castriconi R, Romagnani P, Spaggiari GM, Marcenaro S, Dondero A, *et al.* Expression of the DNAM-1 ligands, Nectin-2 (CD112) and poliovirus receptor (CD155), on dendritic cells: relevance for natural killer-dendritic cell interaction. Blood 2006;107(5):2030-6.
44. Bottino C, Castriconi R, Pende D, Rivera P, Nanni M, Carnemolla B, *et al.* Identification of PVR (CD155) and Nectin-2 (CD112) as cell surface ligands for the human DNAM-1 (CD226) activating molecule. J Exp Med 2003;198(4):557-67.
45. Westin JR, Chu F, Zhang M, Fayad LE, Kwak LW, Fowler N, *et al.* Safety and activity of PD1 blockade by pidilizumab in combination with rituximab in patients with relapsed follicular lymphoma: a single group, open-label, phase 2 trial. Lancet Oncol 2014;15(1):69-77.
46. Matsushita H, Vesely MD, Koboldt DC, Rickert CG, Uppaluri R, Magrini VJ, *et al.* Cancer exome analysis reveals a T-cell-dependent mechanism of cancer immunoediting. Nature 2012;482(7385):400-4.
47. Gubin MM, Zhang X, Schuster H, Caron E, Ward JP, Noguchi T, *et al.* Checkpoint blockade cancer immunotherapy targets tumour-specific mutant antigens. Nature 2014;515(7528):577-81.
48. Ame-Thomas P, Tarte K. The yin and the yang of follicular lymphoma cell niches: role of microenvironment heterogeneity and plasticity. Semin Cancer Biol 2014;24:23-32.
49. Nguyen LT, Ohashi PS. Clinical blockade of PD1 and LAG3 [mdash] potential mechanisms of action. Nat Rev Immunol 2015;15(1):45-56.
50. Lozano E, Dominguez-Villar M, Kuchroo V, Hafler DA. The TIGIT/CD226 axis regulates human T cell function. J Immunol 2012;188(8):3869-75.
51. Joller N, Lozano E, Burkett PR, Patel B, Xiao S, Zhu C, *et al.* Treg cells expressing the coinhibitory molecule TIGIT selectively inhibit proinflammatory Th1 and Th17 cell responses. Immunity 2014;40(4):569-81.
52. Fuhrman CA, Yeh WI, Seay HR, Saikumar Lakshmi P, Chopra G, Zhang L, *et al.* Divergent Phenotypes of Human Regulatory T Cells Expressing the Receptors TIGIT and CD226. J Immunol 2015;195(1):145-55.
53. Locci M, Havenar-Daughton C, Landais E, Wu J, Kroenke MA, Arlehamn CL, *et al.* Human circulating PD-1+CXCR3-CXCR5+ memory Tfh cells are highly functional and correlate with broadly neutralizing HIV antibody responses. Immunity 2013;39(4):758-69.
54. Godefroy E, Zhong H, Pham P, Friedman D, Yazdanbakhsh K. TIGIT-positive circulating follicular helper T cells display robust B-cell help functions: potential role in sickle cell alloimmunization. Haematologica 2015;100(11):1415-25.
55. Pauken KE, Wherry EJ. TIGIT and CD226: tipping the balance between costimulatory and coinhibitory molecules to augment the cancer immunotherapy toolkit. Cancer Cell 2014;26(6):785-7.
56. Guillerey C, Huntington ND, Smyth MJ. Targeting natural killer cells in cancer immunotherapy. Nat Immunol 2016;17(9):1025-36.

57. Weber JS, Yang JC, Topalian SL, Schwartzentruber DJ, White DE, Rosenberg SA. The use of interleukin-2 and lymphokine-activated killer cells for the treatment of patients with non-Hodgkin's lymphoma. J Clin Oncol 1992;10(1):33-40.
58. Liu S, Zhang H, Li M, Hu D, Li C, Ge B, *et al.* Recruitment of Grb2 and SHIP1 by the ITT-like motif of TIGIT suppresses granule polarization and cytotoxicity of NK cells. Cell Death Differ 2013;20(3):456-64.
59. Li M, Xia P, Du Y, Liu S, Huang G, Chen J, *et al.* T-cell immunoglobulin and ITIM domain (TIGIT) receptor/poliovirus receptor (PVR) ligand engagement suppresses interferon-gamma production of natural killer cells via beta-arrestin 2-mediated negative signaling. J Biol Chem 2014;289(25):17647-57.
60. Li W, Whaley CD, Mondino A, Mueller DL. Blocked signal transduction to the ERK and JNK protein kinases in anergic CD4+ T cells. Science 1996;271(5253):1272-6.
61. Adams CL, Grierson AM, Mowat AM, Harnett MM, Garside P. Differences in the kinetics, amplitude, and localization of ERK activation in anergy and priming revealed at the level of individual primary T cells by laser scanning cytometry. J Immunol 2004;173(3):1579-86.
62. Chemnitz JM, Parry RV, Nichols KE, June CH, Riley JL. SHP-1 and SHP-2 associate with immunoreceptor tyrosine-based switch motif of programmed death 1 upon primary human T cell stimulation, but only receptor ligation prevents T cell activation. J Immunol 2004;173(2):945-54.
63. Sheppard KA, Fitz LJ, Lee JM, Benander C, George JA, Wooters J, *et al.* PD-1 inhibits T-cell receptor induced phosphorylation of the ZAP70/CD3zeta signalosome and downstream signaling to PKCtheta. FEBS Lett 2004;574(1-3):37-41.
64. Saunders PA, Hendrycks VR, Lidinsky WA, Woods ML. PD-L2:PD-1 involvement in T cell proliferation, cytokine production, and integrin-mediated adhesion. Eur J Immunol 2005;35(12):3561-9.
65. Kong Y, Zhu L, Schell TD, Zhang J, Claxton DF, Ehmann WC, *et al.* T-Cell Immunoglobulin and ITIM Domain (TIGIT) Associates with CD8+ T-Cell Exhaustion and Poor Clinical Outcome in AML Patients. Clin Cancer Res 2016;22(12):3057-66.

FIGURE LEGENDS

Figure 1. Skewing towards PD-1^{int} phenotype and reduced IFN-γ production in CD8 FL T cells. Single cell suspensions from FL LN and healthy donors (tonsils and PBMC) were analyzed by fluorescence flow cytometry. **A,** CD8 and CD4 T cells were divided into subsets based on expression of PD-1 and ICOS. **B,** Distribution of T-cell subsets gated in (A) in FL (n = 14) compared to tonsils (n = 11) and PBMC (n = 7). **C,** Cells were cultured with or without PMA and ionomycin, and intracellular IFN-γ was measured by flow cytometry. Each data point represents a single donor. FL (n = 9), tonsils (n = 13), PBMC (n = 7). Statistical differences calculated using Mann-Whitney non-parametric test; *p < 0.05, **p < 0.01, ***p < 0.001, ****p < 0.0001.

Figure 2. Intra-tumor FL T cells are distinguished by low levels of TCR-induced distal signaling. Single cell suspensions from FL LN (*n* = 9), and healthy donor tonsils (*n* = 11) and PBMC (*n* = 9) were cultured with or without α-CD3+α-CD28 antibodies for 2 minutes, followed by avidin crosslinking for 1, 4 or 10 minutes and then assayed for TCR-induced phosphorylation of CD3ζ, SLP76 and ERK using phospho-flow cytometry. **A,** Schematic overview of TCR signaling. **B,** Representative histograms of TCR-induced phosphorylation in $CD3^+$ T cells from one FL patient sample compared to one healthy donor tonsil. Shown is median fold change (FC) induction relative to unstimulated cells, using arcsinh transformed data. **C,** TCR-induced p-ERK (4'), p-SLP76 (1') and p-CD3ζ (1') in CD8 and CD4 T-cell subsets shown as median FC induction relative to unstimulated cells. Each data point represents a single donor. Statistical differences calculated using Mann-Whitney non-parametric test; **p* < 0.05, ***p* < 0.01, ****p* < 0.001, *****p* < 0.0001.

Figure 3. Expression patterns of co-inhibitory receptors in CD8 and CD4 T-cell subsets. 11-parameter fluorescence flow cytometry was used to identify co-inhibitory receptor expression in conventional T-cell subsets from FL LN (*n* = 4) and healthy donor tonsils (*n* = 2), using single cell suspensions. Results are visualized by viSNE (gating shown in supplementary Fig. S4). Scale maximum is set to highest measured signal for each marker, or a minimum of 3000. The manually added line in the viSNE plots marks the distinction between CD8 and CD4 T cells.

Figure 4. TIGIT is frequently expressed in FL T_E, T_{EM}, T_{FH} and T_{regs}. Surface expression of co-inhibitory receptors was analyzed in single cell suspensions from FL LN, and healthy donor controls (tonsils and PBMC) by fluorescence flow cytometry. **A,** Plots show $CD3^+$ T cells. **B-C,** Co-inhibitory receptor expression was measured in conventional CD8 and CD4 T-cell subsets. Each data point represents a single donor. FL (*n* = 14), tonsils (*n* = 11), PBMC (*n* = 7). Statistical differences calculated using Mann-Whitney non-parametric test; **p* < 0.05, ***p* < 0.01, ****p* < 0.001 *****p* < 0.0001. **D,** FL LN samples (*n* = 3) were assayed for the contribution of $TIGIT^+$ T_{regs}. Tonsils and PBMC from healthy donors were included for comparison. Bar graph shows mean ± SEM.

Figure 5. TIGIT ligands are expressed in FL and $TIGIT^+$ CD8 T cells are $CD226^{low}$ **A,** FL tissue sections were stained with antibodies against CD155, CD112 and CD21. The tissue sections are closely neighbored to each other, enabling the comparison of identical

structures. Staining pattern of CD155 and CD112 in follicles (arrows) suggests expression by FDC, confirmed by staining of the same follicles with FDC marker CD21. Endothelium (arrow heads) also expressed CD155 and CD112. Image objective x10. **B-C,** TIGIT and CD226 expression was measured in CD8 and CD4 T cells from FL LN (n = 7) using flow cytometry. Healthy donor PBMC was included for comparison. Bargraphs show mean ± SEM. *p < 0.05, **p < 0.01, ***p < 0.001 by Mann-Whitney test.

Figure 6. Dysfunctional TCR distal signaling in FL CD8 TIGIT$^+$ T cells can be restored. Single cell suspensions from FL LN were assayed for TCR-induced signaling and analyzed by phospho-flow cytometry at day 0 and after 48h *in vitro* culture. The cryopreserved cell suspensions contained T cells and tumor cells, while FDC were not detectable in these cultures. Signaling was induced using α-CD3+α-CD28 antibodies for 2 minutes, followed by avidin crosslinking for 1 or 4 minutes, and is shown as median fold change (FC) induction relative to unstimulated cells, using arcsinh transformed data. **A,** TCR-induced p-ERK (4') in TIGIT$^-$ and TIGIT$^+$ CD8 T cells from one representative FL sample at day 0. **B,** Levels of TCR-induced p-ERK (4') and p-SLP76 (1') in CD8 T cells from FL LN (n = 6) at day 0. *p < 0.05 by paired t-test. **C,** Schematic overview of *in vitro* cultures. TCR signaling was induced in single cell suspensions from FL LN at day 0 and after 2 days culture. **D,** TCR-induced signaling was measured in the same FL specimens (n = 4) at day 0 and after 48h *in vitro* culture in the presence of low IL-2. Bar graphs show mean ± SEM. *p < 0.05 by paired t-test. **E-F,** TCR-induced p-ERK (4') was measured in TIGIT$^-$ and TIGIT$^+$ CD8 T cells from the same FL specimens at day 0 and after 48 h *in vitro* culture (in medium only). **E**, Histograms show one representative FL sample. **F,** Recovery of TCR-induced p-ERK by *in vitro* culture shown in TIGIT$^-$ and TIGIT$^+$ CD8 T cells from FL LN (n = 4). **p < 0.01, ****p < 0.0001 by paired t-test.

Author Manuscript Published OnlineFirst on December 7, 2017; DOI: 10.1158/1078-0432.CCR-17-2337
Author manuscripts have been peer reviewed and accepted for publication but have not yet been edited.

Figure 1

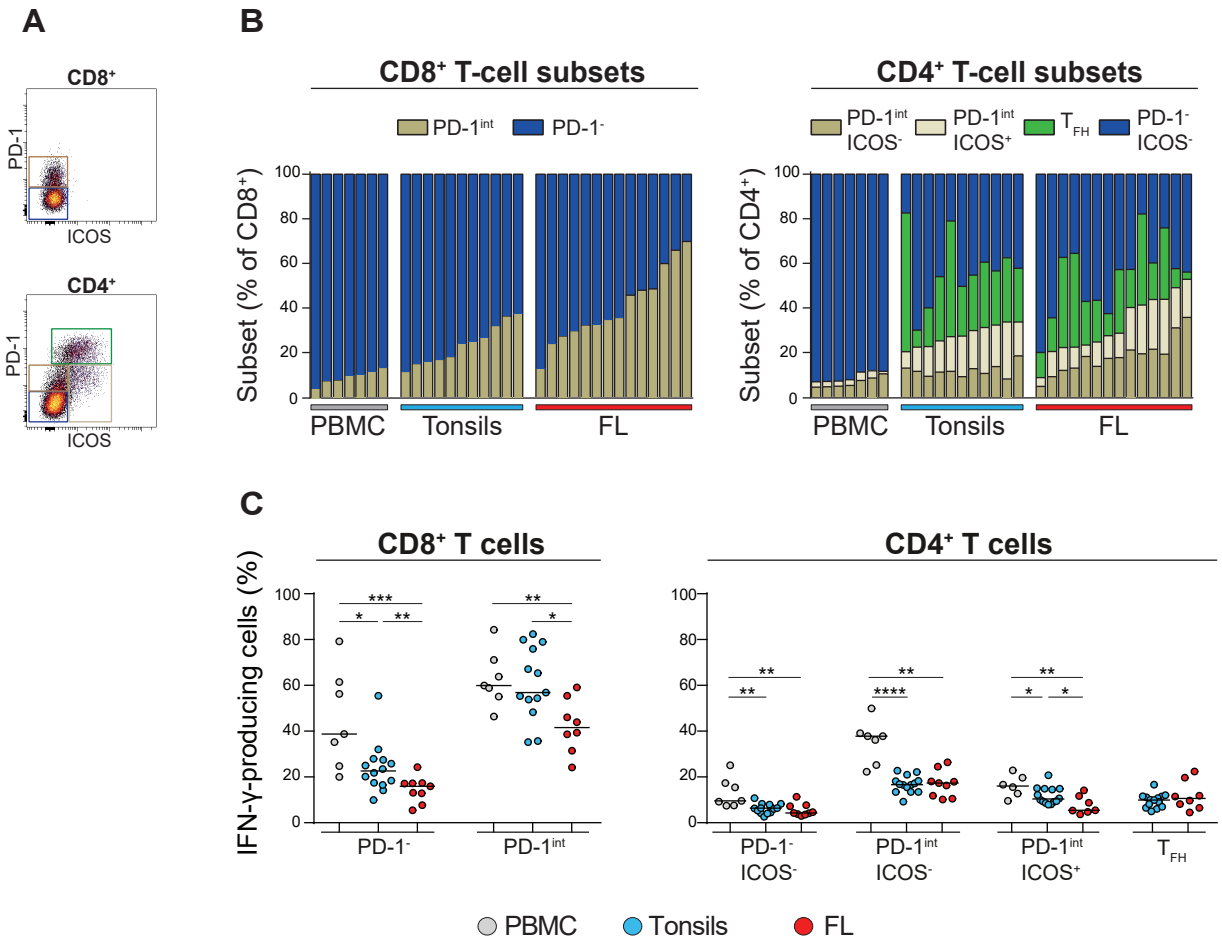

Author Manuscript Published OnlineFirst on December 7, 2017; DOI: 10.1158/1078-0432.CCR-17-2337
Author manuscripts have been peer reviewed and accepted for publication but have not yet been edited.

Figure 2

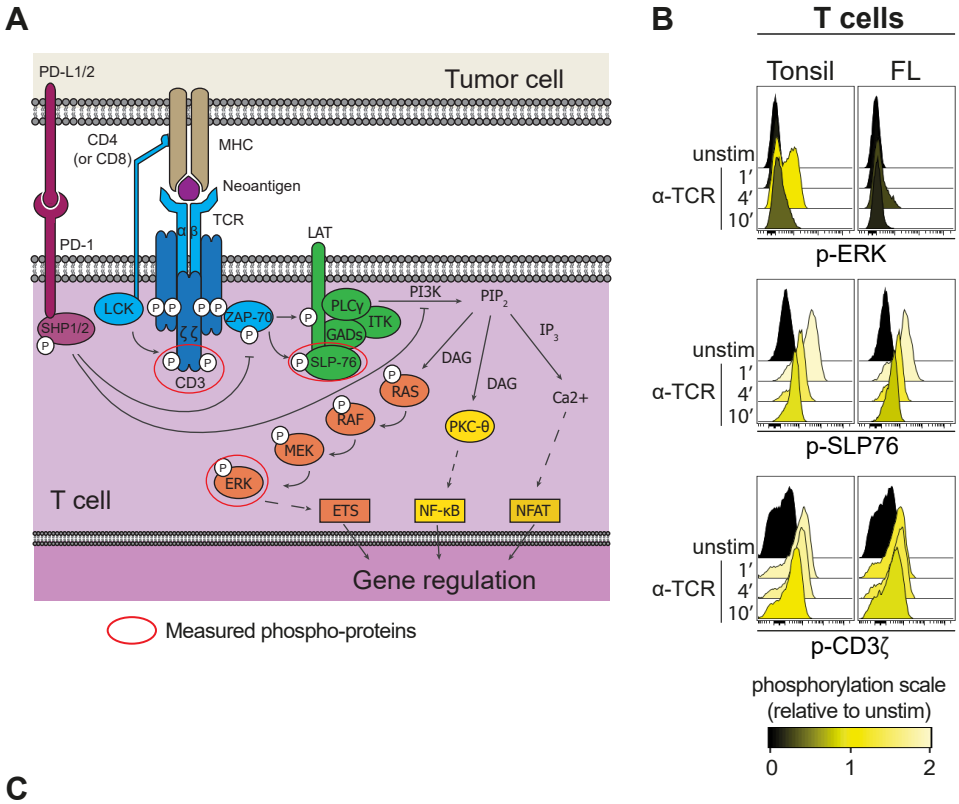

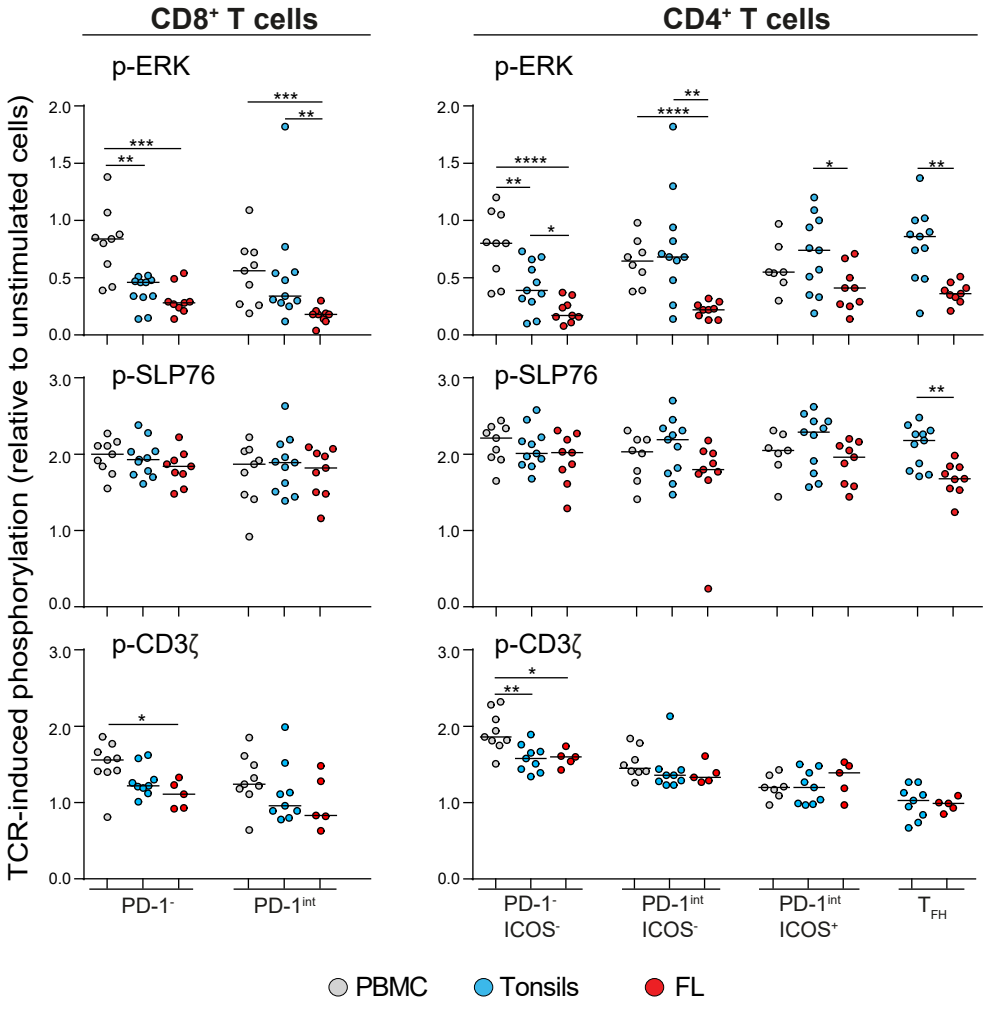

Author Manuscript Published OnlineFirst on December 7, 2017; DOI: 10.1158/1078-0432.CCR-17-2337
Author manuscripts have been peer reviewed and accepted for publication but have not yet been edited.

Figure 3

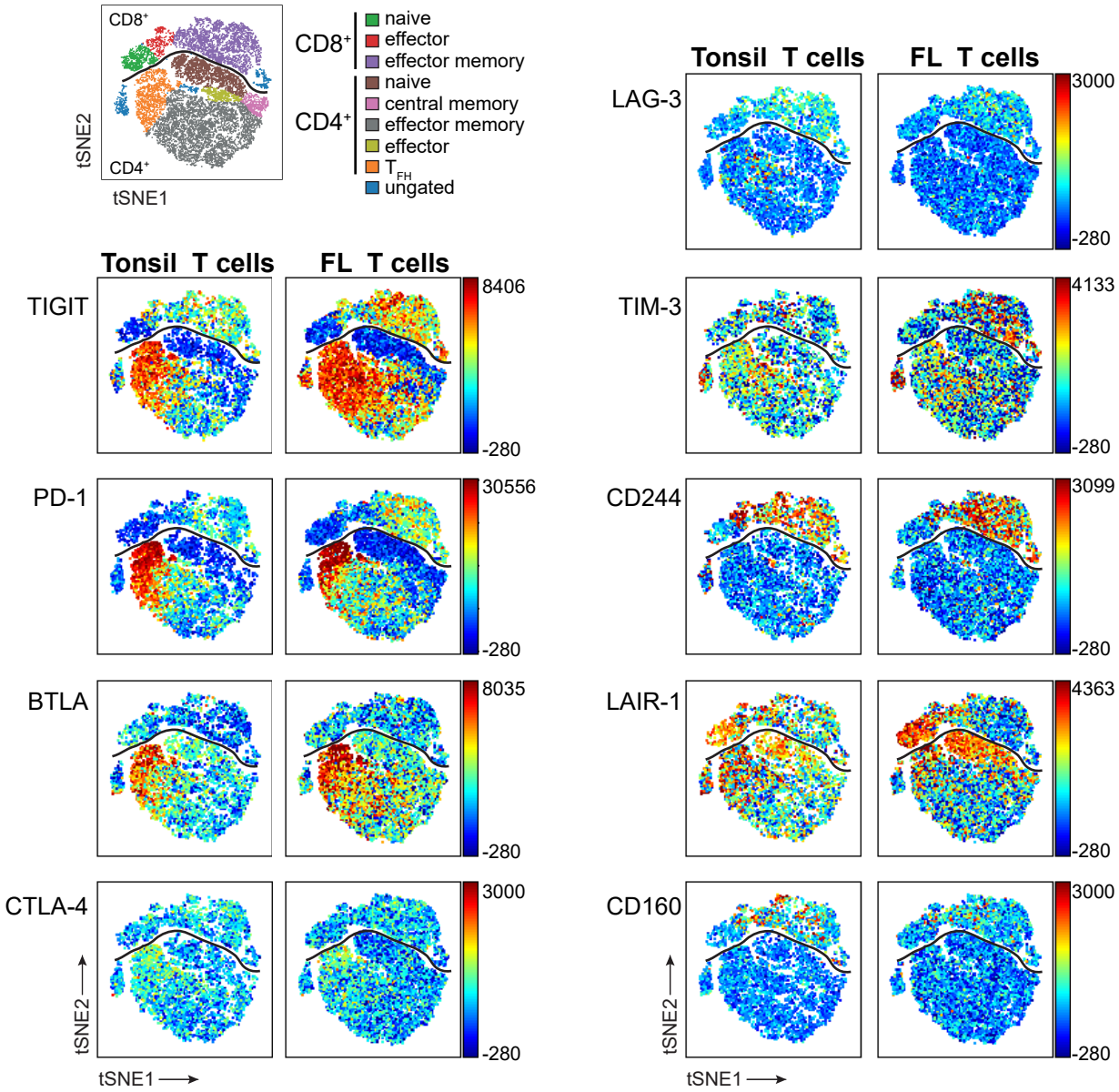

Figure 4

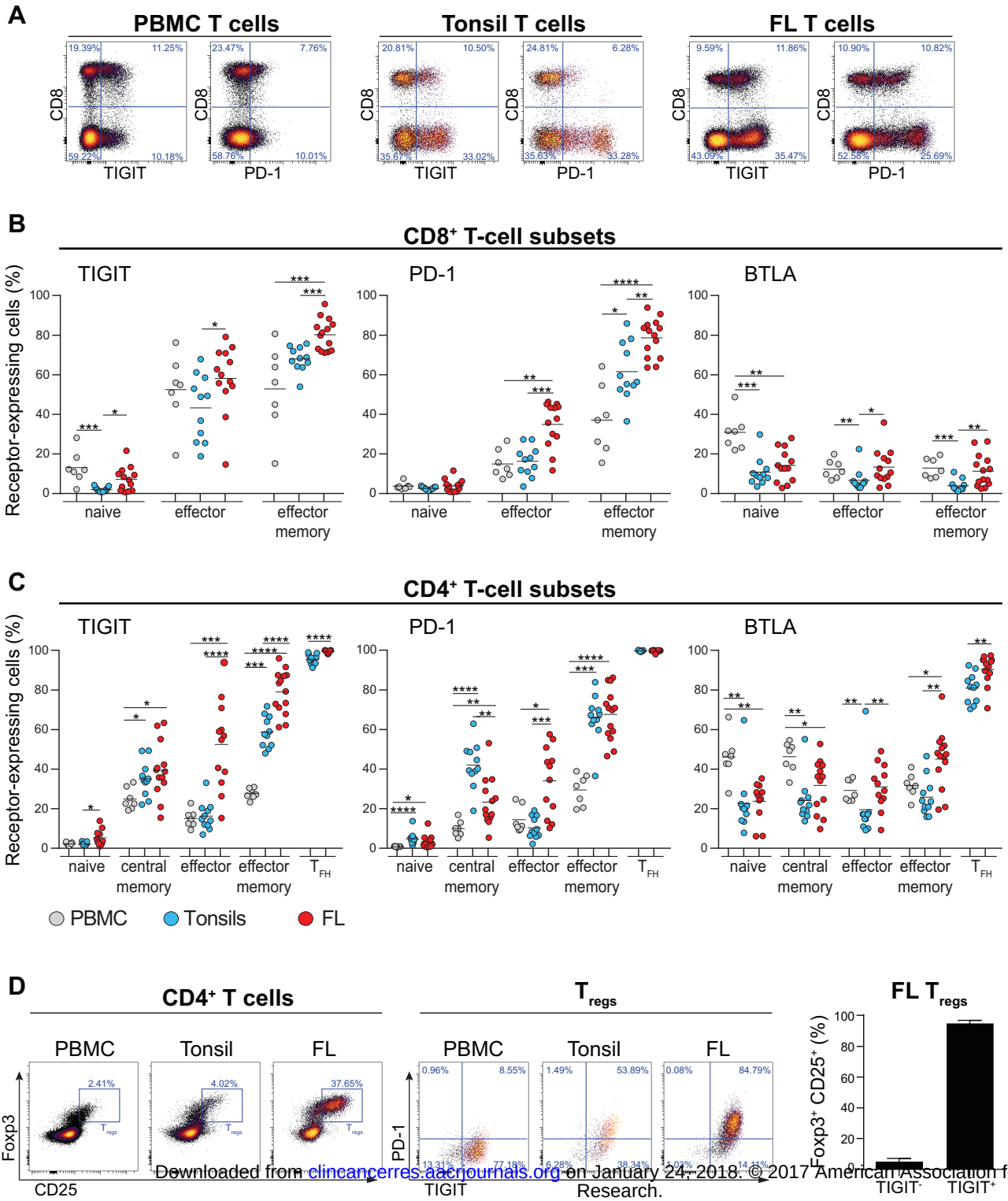

Figure 5

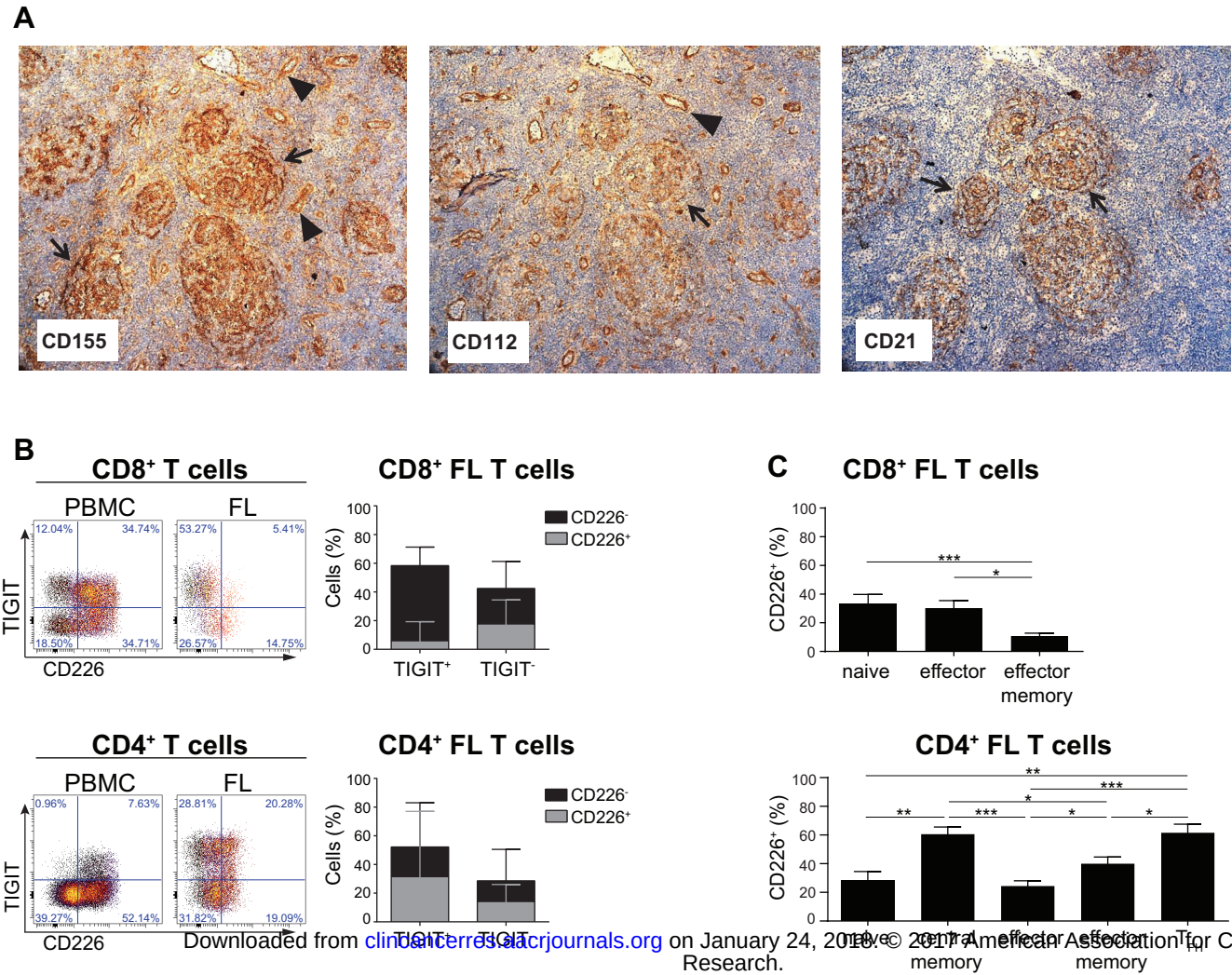

Figure 6

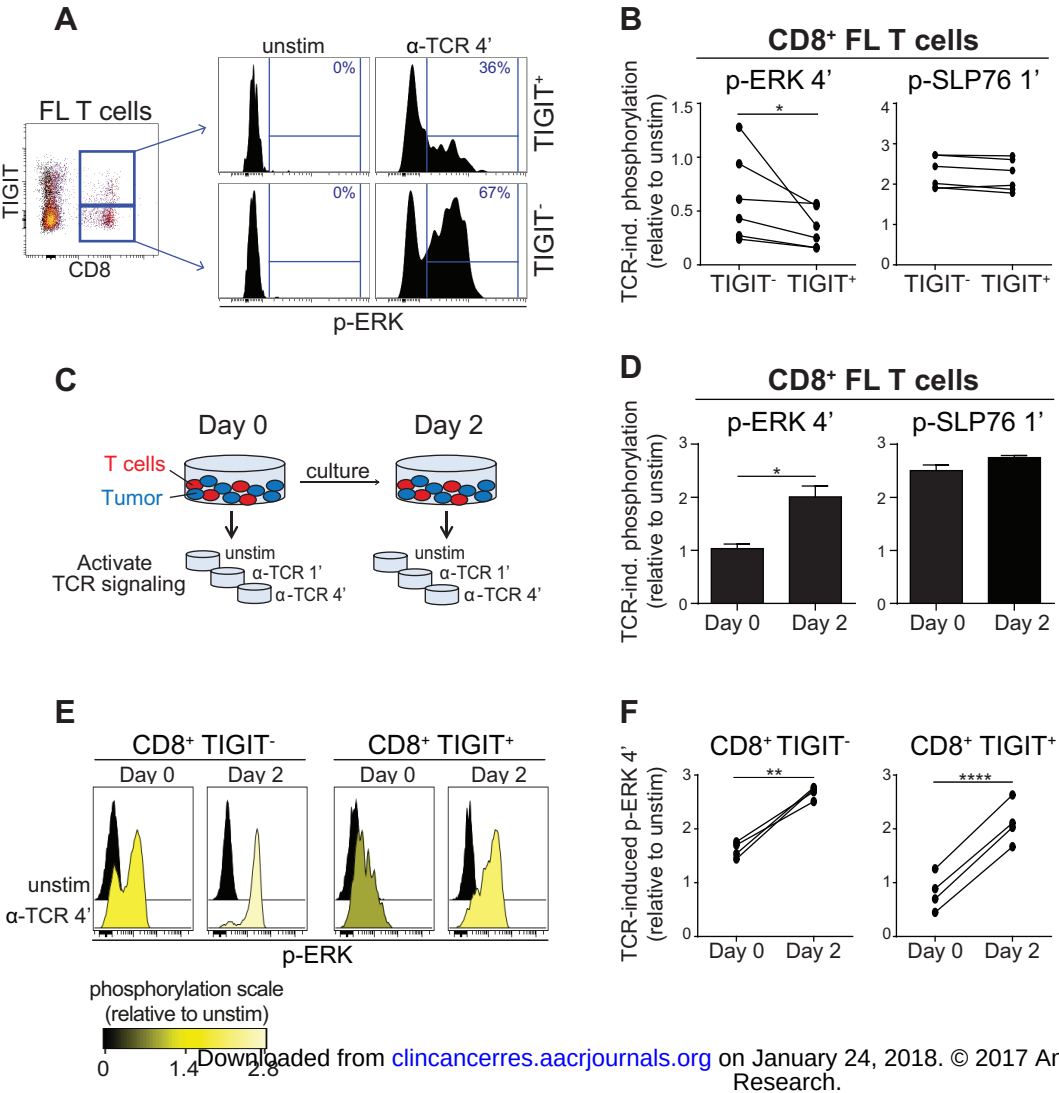

AACR American Association for Cancer Research

Clinical Cancer Research

T cells expressing checkpoint receptor TIGIT are enriched in follicular lymphoma tumors and characterized by reversible suppression of T-cell receptor signaling

Sarah E Josefsson, Kanutte Huse, Arne Kolstad, et al.

Clin Cancer Res Published OnlineFirst December 7, 2017.